Materials Advances

ROYAL SOCIETY OF CHEMISTRY

PAPER

View Article Online
View Journal

Cite this: DOI: 10.1039/d6ma00549g

Ultrasound-assisted one-pot synthesis of tetrazolo[1,5-*a*]pyrimidines and their pharmacological evaluations

Savan S. Bhalodiya,[a] Mehul P. Parmar,[a] Chirag D. Patel,[a] Shana Balachandran,[b] Madan Kumar Arumugam[b] and Hitendra M. Patel*[a]

Received 20th April 2026,
Accepted 18th May 2026

DOI: 10.1039/d6ma00549g

rsc.li/materials-advances

A series of twelve tetrazolo[1,5-*a*]pyrimidine derivatives **4(a–l)** were synthesized *via* an efficient, ultrasound-assisted one-pot multicomponent reaction of 5-aminotetrazole, malononitrile or acetylacetone, and various heterocyclic aromatic aldehydes in acetic acid under ultrasonic conditions. The optimized protocol afforded isolated yields of 85–93% within 12–15 minutes, offering significant advantages over existing methods, including milder conditions, reduced reaction times, and straightforward product isolation without intermediate purification. The synthesized derivatives were evaluated for antimicrobial activity against two Gram-positive bacteria (*Staphylococcus aureus* and *Bacillus subtilis*), two Gram-negative bacteria (*Escherichia coli* and *Klebsiella pneumoniae*), and one pathogenic fungus (*Candida albicans*) using the agar well diffusion method. Compounds **4g** and **4l** demonstrated near-equivalent activity to the aminoglycoside reference gentamicin against *S. aureus*, while compounds **4f**, **4g**, and **4l** exceeded the antifungal reference nystatin against *C. albicans*. The anticancer activity assessed by MTT assay against the HeLa (cervical carcinoma) and HCT-116 (colorectal carcinoma) cell lines revealed that compound **4l** (IC_{50} = 13.4 ± 0.7 μM, HeLa; 22.6 ± 1.1 μM, HCT-116) and compound **4g** outperformed the quercetin reference standard. Structure–activity relationship analysis identified the C-5 acetyl group and benzo[*d*][1,3]dioxol or 5-bromothiophene substituents at C-4 as key contributors to biological potency, establishing **4l** and **4g** as primary lead compounds for further studies.

1. Introduction

Multicomponent reactions (MCRs) are highly valuable in modern synthetic chemistry due to their efficiency, sustainability, and versatility in constructing complex molecules in a single step.[1,2] These reactions adhere to green chemistry principles by often removing the necessity for intermediate purification and minimizing reagent consumption.[3,4] MCRs have broad applications across pharmaceuticals, materials science, and agrochemicals, serving as a robust platform to generate extensive libraries of bioactive compounds, functional materials, and innovative molecular architectures critical for both research progress and industrial use.[5]

Tetrazole and pyrimidine core structures represent highly significant scaffolds in medicinal chemistry, extensively studied for their diverse biological activities and potential in drug design.[6,7] This moiety possesses various biological properties, including antimicrobial,[8,9] anticancer,[10,11] anti-inflammatory,[12,13] anti-oxidant,[14,15] anti-malarial[16,17] and various other properties. Some of the marketed drugs containing tetrazole and pyrimidine are shown in Fig. 1. Extensive research has been conducted in the field of designing and developing biologically active drug molecules, with a primary focus on the molecular hybridization approach.[18,19] This method entails the structural alteration of biologically active pharmacophores to produce hybrid compounds characterized by heightened efficacy and improved activity in comparison to the original parent medications. Moreover, these hybrid pharmaceuticals have demonstrated a unique mechanism of action and a decreased occurrence of undesired side effects when contrasted with their original counterparts.[20,21]

Although several protocols have been reported for the synthesis of tetrazolo-pyrimidine cores using catalysts and media such as PEG-400,[22] TBBDA,[23] MNPs@SiO_2-Pr-AP,[24] $AlCl_3$,[25] [BMIM]BF_4,[26] [BMIM]HSO_4,[27] I_2,[27] PGTSA/Cu(II),[28] *etc.* To the best of our knowledge, there is a lack of alternative methodologies for synthesizing tetrazolo-pyrimidine scaffolds reported in the current literature.[29,30] Therefore, exploring new and diverse strategies for their synthesis remains essential due to their significant importance.

[a] *Department of Chemistry, Sardar Patel University, Vallabh Vidyanagar, Gujarat, 388120, India. E-mail: hm_patel@spuvvn.edu*
[b] *Cancer Biology Lab, Centre for Molecular and Nanomedical Sciences, Sathyabama Institute of Science and Technology, Chennai, Tamil Nadu, 600119, India*

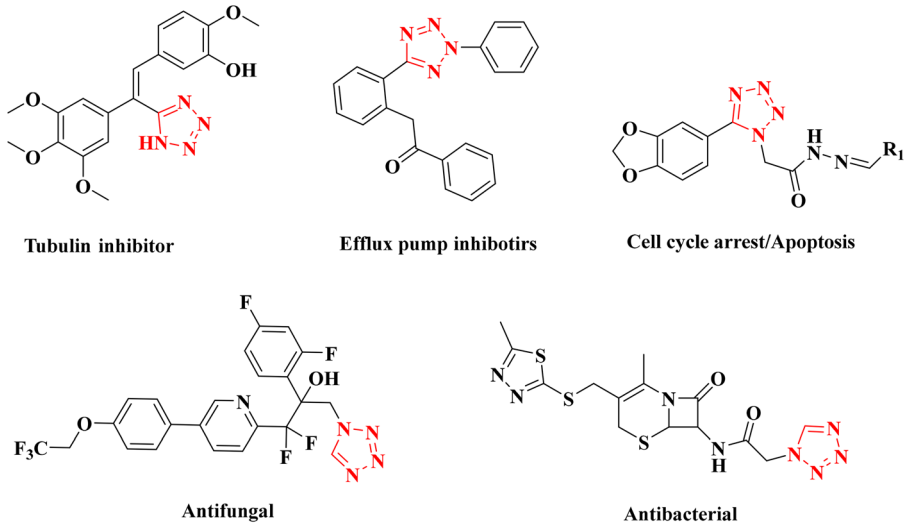

Fig. 1 Tetrazole and pyrimidine-containing marketed drugs.

To the best of our knowledge, this is the first report describing an ultrasound-mediated one-pot synthesis of tetrazolo[1,5-*a*]-pyrimidines. Compared with previously published protocols employing different catalysts, the present methodology offers several distinctive advantages, including being metal free, milder reaction conditions, energy efficiency, significantly higher yields, short reaction time, and simple product isolation. Furthermore, the current work not only provides an environmentally sustainable synthetic route, but also delivers biologically active compounds with promising antimicrobial profiles, thereby demonstrating practical medicinal relevance (Scheme 1).

2. Experimental

2.1. Synthetic protocol for the synthesis of tetrazolo[1,5-*a*]-pyrimidines 4(a–l)

Compounds **4(a–l)** were synthesized *via* an ultrasound-assisted protocol by reacting 5-aminotetrazole (**1**, 1 mmol) with either malononitrile (**2a**, 1 mmol) or acetylacetone (**2b**, 1 mmol) and a range of heterocyclic aromatic aldehydes (**3(a–f)**, 1 mmol) in the presence of acetic acid. The reactions were carried out under ultrasonic irradiation (130 W, 28 kHz) for 12–15 minutes. Reaction progress was periodically checked using thin-layer chromatography (TLC). Upon completion, the reaction mixture was allowed to cool to ambient temperature, and water was added to induce precipitation. The resulting solid product was isolated by filtration, washed with a small quantity of ethanol followed by hot water, and dried to obtain the purified compounds.

2.2. Analytical data of the synthesized compounds 4(a–l)

2.2.1. 5-Amino-7-(5-bromothiophen-2-yl)-4,7-dihydrotetrazolo-[1,5-*a*]pyrimidine-6-carbonitrile (4a). Pale yellow, m.p. 230–232 °C; ^{1}H NMR (DMSO-d$_6$) (d, ppm): 9.51 (s, 1H, NH), 6.76 (d, J = 4Hz, 1H, ArH), 6.68 (d, J = 4Hz, 1H, ArH), 6.59 (s, 2H, NH$_2$), 5.56 (s, 1H, CH); ^{13}C NMR (126 MHz, DMSO-d$_6$) δ: 174.09, 156.82, 144.83, 132.54, 131.41, 121.15, 113.37, 60.93, 53.76; molecular weight: 324.16, MS (ESI m/z): 325.37 [M + H]$^+$; elemental calc. for $C_9H_6BrN_7S$: C-33.35%, H-1.87%, N-30.25%, S-9.89%; found: C-33.38%, H-1.91%, N-30.28%, S-9.92.

2.2.2. 5-Amino-7-(1*H*-imidazol-2-yl)-4,7-dihydrotetrazolo[1,5-*a*]pyrimidine-6-carbonitrile (4b). Pale yellow, m.p. 230–232 °C; ^{1}H NMR (DMSO-d$_6$) (d, ppm): 12.13 (s, 1H, NH), 9.81 (s, 1H, NH), 6.96 (d, J = 4Hz, 1H, ArH), 6.83 (d, J = 4Hz, 1H, ArH), 6.60 (s, 2H, NH$_2$), 5.55 (s, 1H, CH); ^{13}C NMR (126 MHz, DMSO-d$_6$) δ: 172.55, 157.48, 147.79, 121.81, 121.15, 120.73, 60.99, 53.93; Molecular weight:229.21, MS (ESI m/z): 228.52 [M – H]$^-$; elemental calc. for $C_8H_7N_9$: C-41.92%, H-3.08%, N-55.00%; found: C-41.95%, H-3.07%, N-55.03%.

2.2.3. 5-Amino-7-(1*H*-pyrrol-2-yl)-4,7-dihydrotetrazolo[1,5-*a*]-pyrimidine-6-carbonitrile (4c). Pale yellow, m.p. 236–238 °C. ^{1}H NMR (DMSO-d$_6$) (d, ppm): 11.66 (s, 1H, NH), 10.45 (s, 1H, NH), 6.65 (d, J = 4Hz, 1H, ArH), 6.48 (s, 2H, NH$_2$), 6.24 (t, J = 4Hz, 1H, ArH), 6.09 (d, J = 4Hz, 1H, ArH), 5.63 (s, 1H, CH); ^{13}C NMR (126 MHz, DMSO-d$_6$) δ: 173.06, 156.94, 131.41, 119.69, 117.51, 109.19, 107.78, 59.52, 52.23; molecular weight: 228.22, MS (ESI m/z): 229.58[M + H]$^+$; elemental calc. for $C_9H_8N_8$: C-47.37%, H-3.53%, N-49.10%; found: C-47.35%, H-3.55%, N-49.12%.

2.2.4. 5-Amino-7-(1*H*-pyrazol-5-yl)-4,7-dihydrotetrazolo[1,5-*a*]pyrimidine-6-carbonitrile (4d). Pale yellow, m.p. 228–230 °C; ^{1}H NMR (DMSO-d$_6$) (d, ppm): 10.87 (s, 1H, NH), 7.48 (d, J = 4 Hz, 1H, ArH), 6.50 (s, 2H, NH$_2$), 6.08 (d, J = 4 Hz, 1H, ArH), 5.59 (s, 1H, CH); ^{13}C NMR (126 MHz, DMSO-d$_6$) δ: 173.70, 156.30, 145.93, 137.99, 118.66, 104.58, 59.78, 52.61: molecular weight: 229.21, MS (ESI m/z): 228.81 [M − H]$^-$; elemental calc. For $C_8H_7N_9$: C-41.92%, H-3.08%, N-55.00%; found: C-41.89%, H-3.10%, N-55.02%.

2.2.5. 5-Amino-7-(1*H*-imidazol-4-yl)-4,7-dihydrotetrazolo[1,5-*a*]pyrimidine-6-carbonitrile (4e). Pale yellow, m.p. 232–234 °C. ^{1}H NMR (DMSO-d$_6$) (d, ppm): 13.03 (s, 1H, NH), 10.91 (s, 1H, NH), 8.62 (d, J = 4 Hz, 1H, ArH), 7.45 (d, J = 4 Hz, 1H, ArH), 6.49 (s, 2H, NH$_2$), 5.41 (s, 1H, CH); ^{13}C NMR (126 MHz, DMSO-d$_6$) δ: 174.36, 158.60, 137.09, 122.89, 119.81, 117.64, 60.55, 52.87; molecular weight: 229.21, MS (ESI m/z): 230.73 [M + H]$^+$;

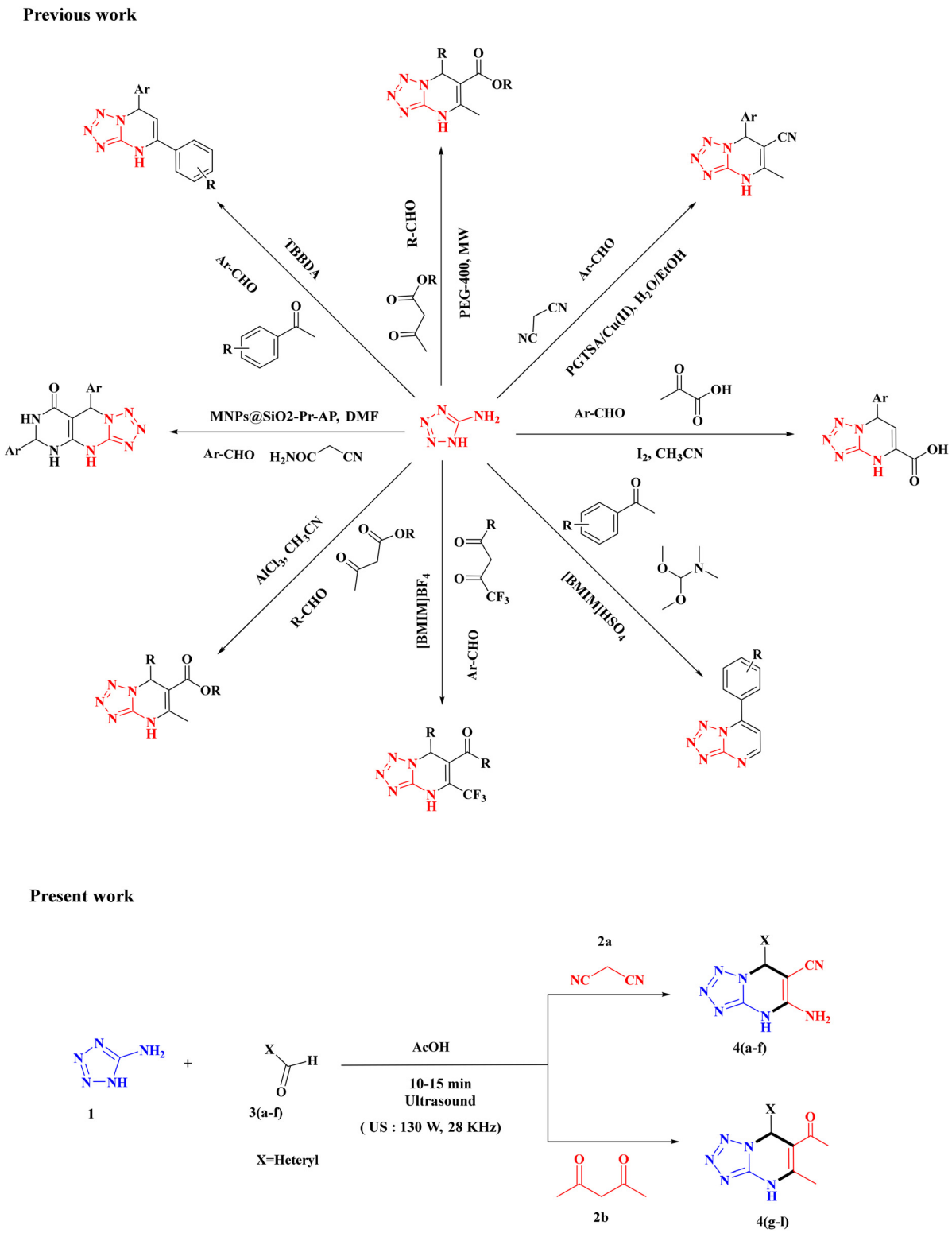

Scheme 1 Reaction protocols of tetrazolo-pyrimidine scaffolds.

elemental calc. for $C_8H_7N_9$: C-41.92%, H-3.08%, N-55.00%; found: C-41.89%, H-3.10%, N-54.95%.

2.2.6. 5-Amino-7-(benzo[*d*][1,3]dioxol-4-yl)-4,7-dihydrotetrazolo-[1,5-*a*]pyrimidine-6-carbonitrile (4f). Pale white crystals, m.p. 238–240 °C. ^{1}H NMR (DMSO-d_6) (d, ppm): 10.92 (s, 1H, NH), 7.08 (d, J = 4 Hz, 1H, ArH), 6.96 (d, J = 4 Hz, 1H, ArH), 6.79 (d, J = 4 Hz, 1H, ArH), 6.49 (s, 2H, NH_2), 6.02 (s, 2H, CH_2), 5.43 (s, 1H, CH); ^{13}C NMR (126 MHz, DMSO-d_6) δ: 172.42, 156.55, 150.54, 149.73, 128.61, 127.54, 125.80, 117.25, 112.96, 101.70, 59.85, 47.23; molecular weight: 283.25, MS (ESI m/z): 282.58 $[M - H]^-$;

elemental calc. for $C_{12}H_9N_7O_2$: C-50.88%, H-3.20%, N-34.62%; found: C-50.90%, H-3.21%, N-34.58%.

2.2.7. 1-(7-(5-Bromothiophen-2-yl)-5-methyl-4,7-dihydrotetrazolo[1,5-*a*]pyrimidin-6-yl)ethan-1-one (4g). Pale white crystals, m.p. 226–228 °C. ^{1}H NMR (DMSO-d_6) (d, ppm): 12.20 (s, 1H, NH), 6.88 (d, J = 4Hz, 1H, ArH), 6.53 (d, J = 4Hz, 1H, ArH), 5.59 (s, 1H, CH), 2.24 (s, 3H, CH_3), 2.02 (s, 3H, CH_3); ^{13}C NMR (126 MHz, DMSO-d_6) δ: 190.70, 156.51, 142.13, 141.07, 129.44, 128.61, 111.95, 109.58, 53.24, 28.19, 17.89; molecular weight: 340.20, MS (ESI m/z): 341.49 $[M + H]^+$; elemental calc. for $C_{11}H_{10}BrN_5OS$: C-38.84%, H-2.96%, N-20.59%, S-9.42%; found: C-38.82%, H-2.99%, N-20.63%, S-9.45%.

2.2.8. 1-(7-(1*H*-Imidazol-2-yl)-5-methyl-4,7-dihydrotetrazolo[1,5-*a*]pyrimidin-6-yl)ethan-1-one (4h). Pale white crystals, m.p. 232–234 °C. ^{1}H NMR (DMSO-d_6) (d, ppm): 13.27 (s, 1H, NH), 12.24 (s, 1H, NH), 7.04 (d, J = 4Hz, 1H, ArH), 6.93 (d, J = 4Hz, 1H, ArH), 5.51 (s, 1H, CH), 2.27 (s, 3H, CH_3), 2.04 (s, 3H, CH_3); ^{13}C NMR (126 MHz, DMSO-d_6) δ: 193.74, 155.51, 148.24, 141.34, 122.03, 121.17, 111.24, 53.54, 27.77, 17.43; molecular weight: 245.25, MS (ESI m/z): 244.24 $[M - H]^-$; elemental calc. for $C_{10}H_{11}N_7O$: C-48.98%, H-4.52%, N-39.98%; found: C-49.02%, H-4.48%, N-39.95%.

2.2.9. 1-(5-Methyl-7-(1*H*-pyrrol-2-yl)-4,7-dihydrotetrazolo[1,5-*a*]pyrimidin-6-yl)ethan-1-one (4i). Pale white crystals, m.p. 226-228 °C. ^{1}H NMR (DMSO-d_6) (d, ppm): 12.39 (s, 1H, NH), 11.16 (s, 1H, NH), 6.64 (d, J = 4Hz, 1H, ArH), 6.16 (d, J = 4Hz, 1H, ArH), 5.96 (d, J = 4Hz, 1H, ArH), 5.51 (s, 1H, CH), 2.20 (s, 3H, CH_3), 2.07 (s, 3H, CH_3); ^{13}C NMR (126 MHz, DMSO-d_6) δ: 194.44, 156.68, 142.34, 130.69, 118.92, 112.13, 108.93, 107.65, 53.89, 27.27, 17.92; molecular weight: 224.26, MS (ESI m/z): 225.44 $[M + H]^+$; elemental calc. for $C_{11}H_{12}N_6O$: C-54.09%, H-4.95%, N-34.41%; found: C-54.06%, H-4.98%, N-34.42%.

2.2.10. 1-(5-Methyl-7-(1*H*-pyrazol-5-yl)-4,7-dihydrotetrazolo[1,5-*a*]pyrimidin-6-yl)ethan-1-one (4j). Pale white crystals, m.p. 232–234 °C. ^{1}H NMR (DMSO-d_6) (d, ppm): 13.18 (s, 1H, NH), 12.39 (s, 1H, NH), 7.09 (d, J = 4 Hz, 1H, ArH), 6.16 (d, J = 4 Hz, 1H, ArH), 5.62 (s, 1H, CH), 2.20 (s, 3H, CH_3), 2.07 (s, 3H, CH_3); ^{13}C NMR (126 MHz, DMSO-d_6) δ: 194.70, 156.68, 144.90, 141.83, 137.22, 111.88, 104.33, 53.38, 27.52, 18.18; molecular weight: 245.25, MS (ESI m/z): 244.87 $[M - H]^-$; elemental calc. for $C_{10}H_{11}N_7O$: C-48.98%, H-4.52%, N-39.98%; found: C-48.95%, H-4.55%, N-40.01%.

2.2.11. 1-(7-(1*H*-Imidazol-4-yl)-5-methyl-4,7-dihydrotetrazolo-[1,5-*a*]pyrimidin-6-yl)ethan-1-one (4k). Pale white crystals, m.p. 230–232 °C. ^{1}H NMR (DMSO-d_6) (d, ppm): 13.06 (s, 1H, NH), 12.36 (s, 1H, NH), 8.74 (d, J = 4 Hz, 1H, ArH), 7.47 (d, J = 4 Hz, 1H, ArH), 5.56 (s, 1H, CH), 2.24 (s, 3H, CH_3), 2.08 (s, 3H, CH_3); ^{13}C NMR (126 MHz, DMSO-d_6) δ: 195.21, 156.42, 141.06, 136.20, 122.76, 119.69, 111.52, 53.38, 27.39, 17.41; molecular weight: 245.25, MS (ESI m/z): 246.29 $[M + H]^+$; elemental calc. for $C_{10}H_{11}N_7O$: C-48.98%, H-4.52%, N-39.98%; found: C-48.94%, H-4.56%, N-39.96%.

2.2.12. 1-(7-(Benzo[*d*][1,3]dioxol-4-yl)-5-methyl-4,7-dihydrotetrazolo[1,5-*a*]pyrimidin-6-yl)ethan-1-one (4l). Pale white crystals, m.p. 234–236 °C. ^{1}H NMR (DMSO-d_6) (d, ppm): 12.36 (s, 1H, NH), 12.39 (s, 1H, NH), 7.13 (d, J = 8 Hz, 1H, ArH), 6.97 (d, J = 8 Hz, 1H, ArH), 6.91 (t, J = 8 Hz, 1H, ArH), 6.05 (s, 2H, CH_2), 5.56 (s, 1H, CH), 2.28 (s, 3H, CH_3), 2.13 (s, 3H, CH_3); ^{13}C NMR (126 MHz, DMSO-d_6) δ: 195.21, 156.42, 151.56, 149.26, 141.06, 125.70, 122.63, 121.48, 112.90, 111.62, 102.02, 48.13, 27.39, 17.41; molecular weight: 299.29, MS (ESI m/z): 298.63 $[M - H]^-$; elemental calc. for $C_{14}H_{13}N_5O_3$: C-56.18%, H-4.38%, N-23.40%; found: C-56.23%, H-4.35%, N-23.38%.

2.3. Biological activity

2.3.1. Antimicrobial activity

2.3.1.1. Test organisms and culture conditions. Five microbial strains were used: two Gram-positive bacteria (*Staphylococcus aureus* and *Bacillus subtilis*), two Gram-negative bacteria (*Escherichia coli* and *Klebsiella pneumoniae*), and one fungus (*Candida albicans*). The bacterial strains were sub-cultured on MHA and incubated at 37 °C for 24 hours. *C. albicans* was maintained on SDA and incubated at 25 °C for 48 h. Suspensions were prepared in sterile normal saline and adjusted to 0.5 McFarland standard ($\sim 1.5 \times 10^8$ CFU mL^{-1}) for bacteria and 1.0×10^6 cells per mL for the fungal strain.

2.3.1.2. Agar well diffusion assay. Antibacterial and antifungal activities were determined by the agar well diffusion method as described in previous reports with some modifications.[31,32] Mueller–Hinton Agar (for bacteria) and Sabouraud Dextrose Agar (for *C. albicans*) were poured into sterile Petri dishes (90 mm) and allowed to solidify. The agar surface was uniformly inoculated by swabbing with the standardised microbial suspension. Wells of 6 mm diameter were bored with a sterile cork borer and 50 μL of each compound solution (100 μg mL^{-1} in 0.1% DMSO) was loaded per well.

Ciprofloxacin (10 μg mL^{-1}) and ampicillin (10 μg mL^{-1}) served as positive antibacterial controls; fluconazole (10 μg mL^{-1}) served as the positive antifungal control; 0.1% DMSO served as the negative control. Plates were pre-incubated at 4 °C for 2 h for prediffusion, then incubated at 37 °C (bacteria, 24 h) or 25 °C (*C. albicans*, 48 h). Zones of inhibition (ZOI) were measured in millimetres including the well diameter using a digital vernier calliper. All experiments were performed in triplicate and the results are expressed as mean ± SD. Statistical analysis was performed by one-way ANOVA with Tukey's *post hoc* test ($p < 0.05$) using GraphPad Prism v9.0.

2.3.1.3. Minimum inhibitory concentration (MIC). MIC values were determined by the broth microdilution method in 96-well plates. Serial two-fold dilutions of each compound (1–512 μg mL^{-1}) were prepared in MHB (bacteria) and RPMI-1640 (fungi). Each well was inoculated with 5×10^5 CFU mL^{-1} and incubated for 18 to 20 h (bacteria, 37 °C) or 24 to 48 h (fungi, 35 °C). Growth was visualised by addition of resazurin (0.015% w/v); a blue-to-pink colour change indicated viable organisms. The MIC was defined as the lowest concentration with no visible colour change. Minimum bactericidal/fungicidal concentrations (MBC/MFC) were determined by sub-culturing MIC and supra-MIC wells onto drug-free agar.

2.3.2. Anticancer activity

2.3.2.1. Cell lines and culture. The HeLa (cervical carcinoma) and HCT-116 (colorectal carcinoma) cell lines were procured

from the National Centre for Cell Science (NCCS), Pune, India. Both cells were maintained in Dulbecco's modified Eagle's medium (DMEM) from Cytiva, USA (Catalog# SH30243.01). The media were supplemented with 10% heat-inactivated Fetal bovine serum (Himedia, Catalog# RM10432), and 1% (v/v) penicillin–streptomycin solution (100 U per mL penicillin and 100 μg per mL streptomycin) (Cytiva, USA. Catalog# SV30010). The cells were maintained at 37 °C in a humidified 5% CO_2 incubator.

2.3.2.2. MTT cell viability assay. The MTT (3-(4,5-dimethylthiazol-2-yl)-2,5-diphenyltetrazolium bromide) assay was performed according to our lab protocol with minimal modifications.[33–35] Cells in the exponential growth phase were seeded at 5×10^3 cells per well in 96-well flat-bottom culture plates (200 μL per well) and incubated for 24 h to allow adhesion. All the test compounds were dissolved in DMSO (10 mM stock) and diluted in complete medium to achieve final concentrations of 0.1, 1, 5, 10, 25, 50, and 100 μM. The cells were treated for 24 h at 37 °C, 5% CO_2. After treatment, the medium was aspirated and 20 μL of MTT reagent (5 mg mL^{-1} in PBS) was added per well, followed by 4 h incubation at 37 °C in the dark. The formazan crystals were solubilised with 100 μL of DMSO per well. Absorbance was recorded at 570 nm on a microplate reader.

Percentage viability was calculated as: % viability = (mean OD treated cells/mean OD control cells) × 100. IC_{50} values were determined by GraphPad Prism. Quercetin was used as a positive reference standard and 0.1% DMSO-treated cells as the negative control. All experiments were conducted in triplicate (n = 3).

2.4. Statistical analysis

All data are expressed as mean ± standard deviation (SD) from three independent experiments (n = 3). Comparisons among groups were performed using one-way analysis of variance (ANOVA) followed by Tukey's multiple comparison test. A p-value < 0.05 was considered statistically significant. Statistical analyses and dose–response curve fitting were performed using GraphPad Prism version 4.0.

3. Results and discussion

3.1. Chemistry

At the beginning of our experiment, we chose 5-amino tetrazole (**1**, 1.0 mmol), malononitrile (**2a**, 1 mmol), and 5-bromo thiophene-2-carboxaldehyde (**3**, 1 mmol) as model substrates to react in a one-pot process. To determine the optimal reaction conditions for reaction, we tested different solvents and catalysts. Our first attempt involved heating the reactants in ethanol without using any catalyst for 24 hours, but it did not result in the desired product (entry 1, Table 1). The model reaction was tested with several different catalysts, as shown in Table 1. Among these, acetic acid in ultrasound worked best, leading to full conversion of the starting materials. Utilizing these best conditions, we did multicomponent reactions with the compounds **1**, **2a**, and **3(a–f)** to check how well and widely this method works. In addition to this, acetyl acetone (**2b**) was used as an active methylene group to enhance the substrate scope. Various heterocyclic aromatic aldehydes reacted smoothly, giving isolated products with moderate to high yields between 76% and 95%. The range of substrates used is detailed in Table 2. Ultrasound irradiation enhances the reaction *via* acoustic cavitation, where collapsing microbubbles create localized high temperature and pressure. This improves mass transfer, increases effective collisions, and accelerates dissolution, leading to faster reactions and higher yields without raising the bulk temperature.[36–38]

Table 1 Optimized reaction conditions for the synthesis of tetrazolo[1,5-*a*]pyrimidine **4a**[a,b]

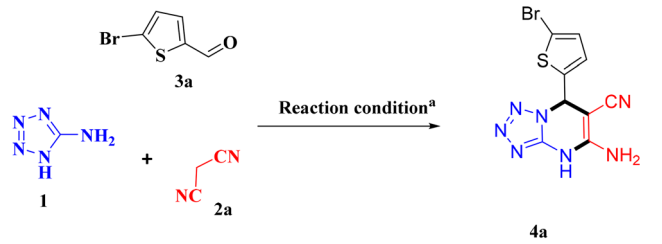

Entry	Catalyst (mol%)	Solvent	Temperature (°C)	Time (min)	Yield (%)[b]
1	—	Ethanol	Reflux	—	—
2	*p*-TSA (20)	Ethanol	Reflux	380	77
3	*p*-TSA (20)	Acetonitrile	Reflux	360	82
4	*p*-TSA (20)	*N*,*N*′-Dimethyl formamide	Reflux	360	85
5	L-Proline (20)	Ethanol	Reflux	400	68
6	L-Proline (20)	Acetonitrile	Reflux	360	59
7	—	Acetic acid	Reflux	320	80
8	—	Ethanol	Ultrasound	—	—
9	*p*-TSA (20)	Ethanol	Ultrasound	15	75
10	L-Proline (20)	Ethanol	Ultrasound	15	86
11	**—**	**Acetic acid**	**Ultrasound**	**12**	**90**

[a] Reaction conditions: 5-amino tetrazole **1** (1.0 mmol), malononitrile **2** (1.0 mmol), and 5 bromo thiophene-2-carbaldehyde **3a** (1.0 mmol). [b] Isolated yield.

Acetic acid acts as both a solvent and proton source, removing the need for additional catalysts or co-solvents. It is considered a green solvent in CHEM21 and GSK guidelines due to its biodegradability, low toxicity, and renewable potential.[39] Acetic acid acts as both a solvent and a Brønsted acid catalyst, providing a polar medium for reactant dissolution and stabilizing intermediates. It activates the aldehyde, promotes enolization of the active methylene compound, and facilitates proton transfer *via* acetate ions. It is regenerated, confirming its catalytic role.[40]

As an example, the synthesis of compound **4a** was confirmed by seeing a signal singlet at 5.56 ppm in the ^{1}H-NMR spectrum. The key points were that there were no signals for the methylene protons from malononitrile and no signal for the aldehyde proton. Also, the lack of a signal for the aldehyde carbon at 200 ppm in the ^{13}C-NMR spectrum helped to prove that the compound was formed.

To demonstrate the scalability of the developed protocol, a gram scale reaction was performed using 5-amino tetrazole (**1**), malononitrile (**2a**), and 5-bromo thiophene-2-carboxaldehyde (**3a**) at 5 mmol scale under the optimized conditions. The reaction

Table 2 Substrate scope for tetrazolo[1,5-*a*]pyrimidines **4(a–l)**[a]

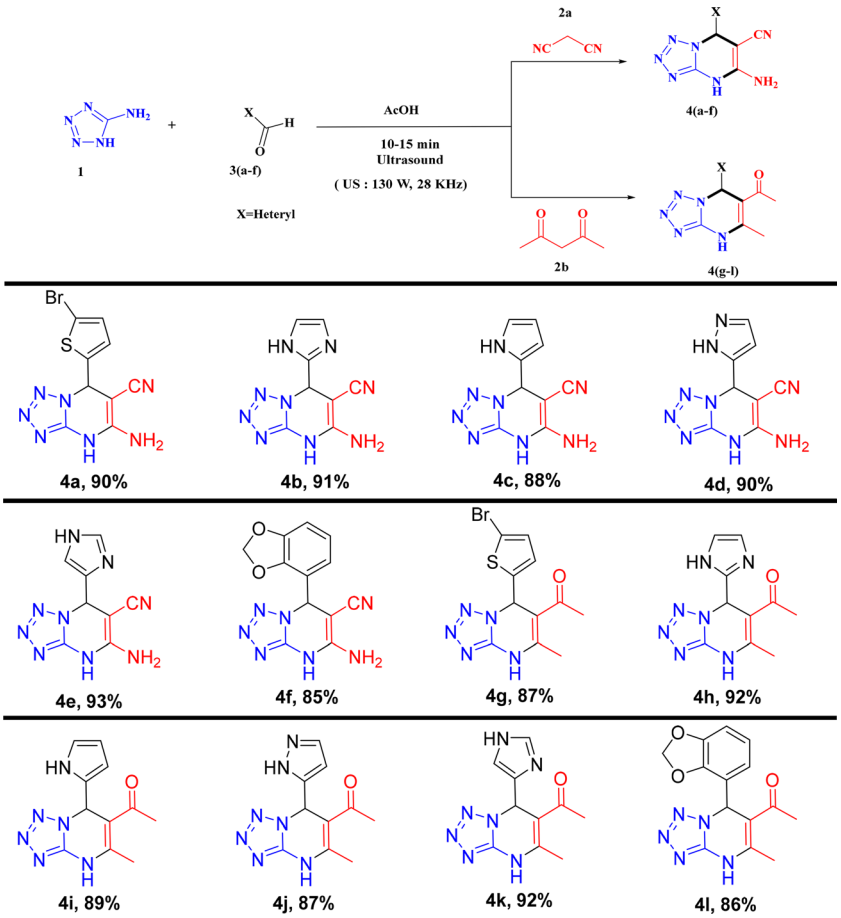

[a] Reaction conditions: 5-amino tetrazole **1** (1.0 mmol), malononitrile **2a**/acetyl acetone **2b** (1.0 mmol), and heterocyclic aromatic aldehyde **3(a–f)** (1.0 mmol); 4 ml acetic acid, ultrasound.

afforded 1.442 g (89% yield) of the desired product without any significant decrease in yield or increase in reaction time, confirming the practical utility and scalability of the present methodology.

3.2. Biological activity

3.2.1. Antimicrobial activity. The antimicrobial activity of the synthesized tetrazolo[1,5-*a*]pyrimidine derivatives **4(a–l)** was evaluated against two Gram-positive bacteria (*Staphylococcus aureus* and *Bacillus subtilis*), two Gram-negative bacteria (*Escherichia coli* and *Klebsiella pneumoniae*), and one pathogenic fungus (*Candida albicans*) by the agar well diffusion method at 100 μg mL^{-1}. Gentamicin (10 μg mL^{-1}) and chloramphenicol (5 μg mL^{-1}) served as antibacterial reference standards; nystatin (10 μg mL^{-1}) served as the antifungal reference. The results, expressed as zone of inhibition (ZOI, mm; mean ± SD, $n = 3$), are presented in Table 3.

All twelve compounds demonstrated measurable inhibitory activity against all five tested organisms, confirming that the tetrazolo[1,5-*a*]pyrimidine scaffold carries intrinsic broad-spectrum antimicrobial pharmacophoric character. Gram-positive organisms were consistently more susceptible than Gram-negative strains across the entire series, a pattern well-documented for N-heterocyclic compounds and attributable to the additional permeability barrier conferred by the outer membrane of Gram-negative bacteria.

Compounds **4f** (19.2 ± 0.7 mm), **4g** (20.6 ± 0.6 mm), **4j** (18.8 ± 0.6 mm), and **4l** (21.4 ± 0.7 mm) all surpassed standard chloramphenicol against *S. aureus*, with **4l** recording the highest ZOI of all the compounds. Against *B. subtilis*, **4g** (19.6 ± 0.5 mm) and **4l** (20.2 ± 0.6 mm) exceeded the chloramphenicol reference value (17.8 ± 0.5 mm), further affirming the potency of the acetyl subseries. Against Gram-negative strains, **4l** (18.2 ± 0.6 mm against *E. coli*) demonstrates that activity extends meaningfully beyond Gram-positive selectivity.

When compared to gentamicin (21.6 ± 0.6 mm, *S. aureus*), compound **4l** (21.4 ± 0.7 mm) achieved near-equivalent activity, a significant finding for a first-generation unoptimised synthetic scaffold. Compound **4g** (20.6 ± 0.6 mm) was likewise closely comparable. These observations suggest that the tetrazolopyrimidine core, particularly when bearing a bromothiophene or benzo[*d*][1,3]dioxol substituent at C-7, achieves a level of antibacterial potency ordinarily associated with aminoglycoside-class reference agents.

In the antifungal results against *C. albicans*, three compounds **4f** (15.8 ± 0.6 mm), **4g** (16.4 ± 0.5 mm), and **4l**(17.6 ± 0.6 mm)

Table 3 Antimicrobial activity - zone of inhibition (mm) at 100 μg mL^{-1}

	Gram-positive		Gram-negative		Fungal
	S. aureus	*B. subtilis*	*E. coli*	*K. pneumoniae*	*C. albicans*
4a	**18.4 ± 0.6**	**17.1 ± 0.7**	14.2 ± 0.5	13.5 ± 0.5	12.6 ± 0.4
4b	16.2 ± 0.5	15.6 ± 0.6	13.8 ± 0.6	12.8 ± 0.4	11.4 ± 0.5
4c	14.8 ± 0.4	14.2 ± 0.5	12.6 ± 0.4	11.6 ± 0.3	10.2 ± 0.4
4d	17.6 ± 0.5	16.4 ± 0.4	15.0 ± 0.5	13.9 ± 0.5	13.2 ± 0.4
4e	16.8 ± 0.6	15.8 ± 0.5	14.4 ± 0.5	13.2 ± 0.4	12.0 ± 0.5
4f	19.2 ± 0.7	18.4 ± 0.6	16.8 ± 0.6	15.4 ± 0.5	15.8 ± 0.6
4g	20.6 ± 0.6	19.6 ± 0.5	17.4 ± 0.5	16.2 ± 0.5	16.4 ± 0.5
4h	17.4 ± 0.5	16.8 ± 0.6	14.8 ± 0.4	13.8 ± 0.4	12.8 ± 0.5
4i	15.6 ± 0.4	14.8 ± 0.5	13.2 ± 0.5	12.2 ± 0.5	10.8 ± 0.4
4j	**18.8 ± 0.6**	17.6 ± 0.6	**16.2 ± 0.5**	**14.8 ± 0.4**	14.6 ± 0.5
4k	17.8 ± 0.5	16.6 ± 0.5	15.4 ± 0.6	14.2 ± 0.5	13.4 ± 0.5
4l	**21.4 ± 0.7**	**20.2 ± 0.6**	**18.2 ± 0.6**	17.0 ± 0.5	**17.6 ± 0.6**
Gentamicin	21.6 ± 0.6	20.4 ± 0.6	19.0 ± 0.5	18.2 ± 0.5	—
Chloramphenicol	18.6 ± 0.5	17.8 ± 0.5	15.2 ± 0.5	14.6 ± 0.4	—
Nystatin	—	—	—	—	14.8 ± 0.4

Positive controls: chloramphenicol (5 μg mL^{-1}), gentamicin (10 μg mL^{-1}), nystatin (10 μg mL^{-1}). Values are mean ± SD of three independent experiments (mean ± SD, n = 3).

exceeded the nystatin reference standard (14.8 ± 0.4 mm at 10 μg mL^{-1}), with **4l**showing an 18.9% higher ZOI than the standard compound. The methylenedioxy group present in **4f** and **4l** may facilitate interaction with fungal membrane ergosterol or cell wall biosynthetic enzymes, warranting further mechanistic investigation.

The acetyl sub-series (**4g–4l**) demonstrated consistently superior activity compared to the carbonitrile sub-series (**4a–4f**) across all organisms, suggesting that the acetyl group at C-5 plays a favourable role in target engagement or cellular permeability. The benzo[*d*][1,3]dioxol substituent (**4f**, **4l**) and the 5-bromothiophene moiety (**4a**, **4g**) consistently produced the highest activity, whereas pyrrol-2-yl-bearing compounds **4c** and **4i** showed low Zone of Inhibition, indicating the importance of substituent lipophilicity and electronic character at C-4 for antimicrobial potency.

The antimicrobial activity of the synthesized tetrazolo[1,5-*a*]pyrimidine derivatives 4(a–l) was evaluated against Gram-positive bacteria (*Staphylococcus aureus* and *Bacillus subtilis*), Gram-negative bacteria (*Escherichia coli* and *Klebsiella pneumoniae*), and the fungal strain *Candida albicans* using the broth dilution method. The minimum inhibitory concentration (MIC) values are presented in Table 4.

Among the synthesized derivatives, compounds **4f** and **4i** exhibited the most potent and broad-spectrum antimicrobial activity with lower MIC values against all tested microbial strains. Compound **4f** showed excellent inhibitory activity against *S. aureus*, *B. subtilis*, *E. coli*, and *C. albicans* with MIC values of 3.12 μg mL^{-1}, while a slightly higher MIC value of 6.25 μg mL^{-1} was observed against *K. pneumoniae*. Similarly, compound **4i** demonstrated strong antimicrobial efficacy with MIC values of 3.12 μg mL^{-1} against *S. aureus*, *B. subtilis*, *E. coli*, and *C. albicans*. Compounds **4g**, **4h**, and **4j** also displayed promising antibacterial activity, particularly against *E. coli*, with MIC values of 3.12 μg mL^{-1}. Compound **4g** further exhibited significant antifungal activity against *C. albicans* with an MIC value of 3.12 μg mL^{-1}. In contrast, compound **4k** showed comparatively weaker antimicrobial activity with higher MIC values ranging from 12.5 to 25 μg mL^{-1} against all tested strains.

Table 4 MICs of the synthesized tetrazolo[1,5-*a*]pyrimidine derivatives **4(a–l)** (μg mL^{-1})

	Gram-positive		Gram-negative		Fungal
	S. aureus	*B. subtilis*	*E. coli*	*K. pneumoniae*	*C. albicans*
4a	**3.12**	**6.25**	12.5	6.25	12.5
4b	**3.12**	3.12	6.25	6.25	12.5
4c	**3.12**	**6.25**	12.5	6.25	12.5
4d	**3.12**	**3.12**	25	25	12.5
4e	6.25	12.5	12.5	12.5	6.25
4f	**3.12**	**3.12**	**3.12**	**6.25**	**3.12**
4g	**3.12**	**6.25**	**3.12**	**6.25**	**3.12**
4h	6.25	**3.12**	**3.12**	**6.25**	6.25
4i	**3.12**	**3.12**	**3.12**	**6.25**	**3.12**
4j	**3.12**	**12.5**	**3.12**	**6.25**	**3.12**
4k	12.5	**12.5**	**25**	**25**	25
4l	**3.12**	**3.12**	**6.5**	25	**12.5**
Gentamicin	10	10	10	10	—
Chloramphenicol	5	5	5	5	—
Nystatin	—	—	—	—	10

Gram-positive bacterial strains were generally more susceptible to the synthesized compounds compared to Gram-negative strains. Most derivatives demonstrated moderate to strong inhibitory activity against *S. aureus* and *B. subtilis*, with MIC values predominantly in the range of 3.12–6.25 μg mL^{-1}. However, certain compounds such as 4d and 4k exhibited reduced activity against Gram-negative bacteria, especially *E. coli* and *K. pneumoniae*, with MIC values of 25 μg mL^{-1}. The antifungal screening against *Candida albicans* revealed that compounds **4f**, **4g**, **4i**, and **4j** possessed remarkable antifungal activity with MIC values of 3.12 μg mL^{-1}, which was superior to the standard antifungal drug nystatin (10 μg mL^{-1}). Overall, the synthesized tetrazolo[1,5-*a*]pyrimidine derivatives demonstrated significant antimicrobial potential, with compounds **4f** and **4i** emerging as the most active candidates for further pharmacological investigation.

Table 5 Anticancer activity – IC_{50} values (μM) against the HeLa and HCT-116 cell lines

Compd.	IC_{50} (μM) mean ± SD (n = 3) HeLa (cervical carcinoma)	HCT-116 (colorectal carcinoma)
4a	24.8 ± 1.1	35.2 ± 1.4
4b	31.2 ± 1.3	40.6 ± 1.5
4c	38.6 ± 1.5	48.2 ± 1.6
4d	27.2 ± 1.2	37.8 ± 1.5
4e	29.8 ± 1.3	39.4 ± 1.4
4f	19.6 ± 0.9	29.4 ± 1.3
4g	**15.8 ± 0.8**	**25.6 ± 1.2**
4h	28.4 ± 1.2	38.2 ± 1.4
4i	36.8 ± 1.4	46.4 ± 1.6
4j	22.4 ± 1.0	32.4 ± 1.3
4k	26.0 ± 1.1	36.0 ± 1.4
4l	**13.4 ± 0.7**	**22.6 ± 1.1**
QCT	18.8 ± 0.9	30.2 ± 0.8

Reference standard drug; QCT = Quercetin. IC_{50} = concentration causing 50% inhibition of cell growth determined from dose–response curves (0.1–100 μM). Values are mean ± SD of three independent experiments

3.3. Anticancer activity

The cytotoxic activity of compounds **4(a–l)** was evaluated against the HeLa (cervical carcinoma) and HCT-116 (colorectal carcinoma) cell lines using the MTT assay after 24 h compound treatment. The IC_{50} values (μM; mean ± SD, n = 3) were determined from dose–response curves (0.1–100 μM) and are presented in Table 5. Quercetin (QCT) was used as the reference standard.

All twelve synthesised compounds demonstrated dose-dependent antiproliferative activity against both cell lines, with IC_{50} values ranging from 13.4 to 38.6 μM (HeLa) and 22.6 to 48.2 μM (HCT-116). Compound **4l** showed IC_{50} values of 13.4 ± 0.7 μM (HeLa) and 22.6 ± 1.1 μM (HCT-116) the best performance of the compounds. Compound **4g** similarly outperformed quercetin with IC_{50} values of 15.8 ± 0.8 μM (HeLa) and 25.6 ± 1.2 μM (HCT-116). Compound **4f** (HeLa IC_{50}: 19.6 ± 0.9 μM) was comparable to the quercetin reference value, differing by less than one standard deviation. Compound **4j** also performed well against HeLa cells (22.4 ± 1.0 μM), approaching quercetin-level activity.

HeLa cells were consistently more sensitive than HCT-116 cells across the entire compound series, suggesting differential susceptibility possibly linked to the higher baseline proliferative rate and distinct metabolic profile of cervical carcinoma cells. Compounds **4c** and **4i** exhibited the weakest cytotoxicity (IC_{50} > 36 μM in both lines), mirroring their comparatively lower antimicrobial activity and suggesting a converging structure–activity relationship across both biological assays.

The benzo[*d*][1,3]dioxol substituent at C-4, present in **4f** and **4l**, consistently drove the highest potency, consistent with the known role of the methylenedioxy pharmacophore in natural product-derived anticancer agents such as piperlongumine and podophyllotoxin. The bromothiophene moiety in **4g** contributed to enhanced cellular activity, likely through increased lipophilicity and membrane permeability facilitating intracellular accumulation. The acetyl sub-series (**4g–4l**) demonstrated overall superior activity reinforcing the conclusion that the C-5 acetyl group modulates cytotoxic potency favourably. These findings collectively identify **4l** and **4g** as the primary lead compounds from this scaffold for further anticancer optimisation, with rational structural modifications at the C-4 aryl position offering a direct pathway toward enhanced potency.

4. Conclusion

In summary, an ultrasound-mediated one-pot multicomponent strategy was successfully developed for the synthesis of tetrazolo[1,5-*a*]pyrimidine derivatives using acetic acid as a green, catalyst-free reaction medium. This approach represents the first reported ultrasound-assisted protocol for this scaffold and delivers superior performance over conventional methods in terms of reaction time (12–15 min), product yield (76–95%), and operational simplicity. The broad substrate scope, encompassing diverse heterocyclic aromatic aldehydes with both malononitrile and acetylacetone as active methylene components, underscores the versatility and generality of the methodology. Biological evaluation across twelve synthesized derivatives revealed broad-spectrum antimicrobial activity against all tested organisms. The acetyl sub-series (**4g–4l**) consistently outperformed the carbonitrile sub-series (**4a–4f**), confirming that the C-5 acetyl group plays a beneficial role in target engagement. Among the tested compounds, **4l** and **4g** – bearing the benzo[*d*][1,3]dioxol and 5-bromothiophene substituents at C-4, respectively – emerged as the most potent antimicrobial agents with minimal concentrations, with activity approaching that of the clinical reference gentamicin against *S. aureus* and surpassing nystatin against *C. albicans*. Anticancer screening further validated these leads, with **4l** and **4g** achieving IC_{50} values superior to the quercetin reference against both the HeLa and HCT-116 cell lines. The convergent structure–activity relationship observed across both biological assays highlights the central pharmacophoric importance of the methylenedioxy and bromothiophene groups at C-4. These findings establish the tetrazolopyrimidine scaffold as a promising platform for the development of novel antimicrobial and anticancer agents, warranting further mechanistic investigation and structural optimization. The current study is limited by the absence of normal-cell cytotoxicity analysis and selectivity index evaluation. Future investigations will include normal human cell lines to assess the safety and selectivity of the synthesized compounds for potential therapeutic applications.

Author contributions

Savan S. Bhalodiya: method development, investigation, validation, spectral analysis, writing an original draft, Mehul P. Parmar: writing – review editing, spectral analysis, Shana Balachandran: investigation, biological study, writing – review and editing, formal analysis, Chirag D. Patel: writing – review and editing, formal analysis, Madan Kumar Arumugam: biological study, writing – review and editing, formal analysis, Hitendra M. Patel: writing –

review and editing, supervision, method development, investigation, formal analysis, conceptualization.

Conflicts of interest

The authors declare no conflict of interest.

Data availability

The data supporting this article have been included as part of the Supplementary Information (SI). Supplementary information is available. See DOI: https://doi.org/10.1039/d6ma00549g.

Acknowledgements

The authors would like to extend their heartfelt gratitude to the Department of Chemistry, Sardar Patel University, Vallabh Vidyanagar for providing the necessary research facilities. SSB is thankful for the CSIR-NET fellowship (Reference No.: Nov/06/2020(i)EU-V). MPP is thankful to the Knowledge Consortium of Gujarat for the SHODH fellowship (Student Reference No.: 2021016434). CDP is thankful to the National fellowship for scheduled Tribe (Award No.: 202223-NFST-GUJ-00003).

References

1 R. Javahershenas, J. Han, M. Kazemi and P. J. Jervis, Recent Advances in the Multicomponent Synthesis of Heterocycles using Thiosemicarbazide, *ChemistrySelect*, 2024, **9**(30), e202401496.
2 P. J. Patel, R. M. Vala, S. G. Patel, D. B. Upadhyay, D. P. Rajani, F. Damiri, M. Berrada and H. M. Patel, Catalyst-free synthesis of imidazo[5,1-b]quinazolines and their antimicrobial activity, *J. Mol. Struct.*, 2023, **1285**, 135467.
3 R. Javahershenas, J. Han, M. Kazemi and P. J. Jervis, Recent Advances in the Application of 2-Aminobenzothiazole to the Multicomponent Synthesis of Heterocycles, *ChemistryOpen*, 2024, **13**(11), e202400185.
4 R. Javahershenas and S. Nikzat, Recent advances in the multicomponent synthesis of heterocycles using tetronic acid, *RSC Adv.*, 2023, **13**(24), 16619–16629.
5 S. S. Bhalodiya, M. P. Parmar, C. D. Patel, S. G. Patel, D. P. Vala, N. Suresh, B. Jayachandran, M. Kumar Arumugam, M. Narayan and H. M. Patel, Acetic Acid-Driven One-Pot Synthesis of 4,7-dihydro-[1,2,3]thiadiazolo[5,4-*b*]pyridine-6-carboxamides and Pharmacological Evaluations, *ChemMedChem*, 2025, **20**(2), e202400595.
6 N. Kaushik, N. Kumar, A. Kumar and U. K. Singh, Tetrazoles: Synthesis and Biological Activity, *Immunol., Endocr. Metab. Agents Med. Chem.*, 2018, **18**(1), 3–21.
7 E. Zarenezhad, M. Farjam and A. Iraji, Synthesis and biological activity of pyrimidines-containing hybrids: Focusing on pharmacological application, *J. Mol. Struct.*, 2021, **1230**, 129833.
8 S. A. F. Rostom, H. M. A. Ashour, H. A. A. E. Razik, A. E. F. H. A. E. Fattah and N. N. El-Din, Azole antimicrobial pharmacophore-based tetrazoles: Synthesis and biological evaluation as potential antimicrobial and anticonvulsant agents, *Bioorg. Med. Chem.*, 2009, **17**(6), 2410–2422.
9 A. H. Moustafa, H. A. Saad, W. S. Shehab and M. M. El-Mobayed, Synthesis of Some New Pyrimidine Derivatives of Expected Antimicrobial Activity, *Phosphorus, Sulfur Silicon Relat. Elem.*, 2007, **183**(1), 115–135.
10 A.-G. E. Amr, A. M. Mohamed, S. F. Mohamed, N. A. Abdel-Hafez and A. E.-F. G. Hammam, Anticancer activities of some newly synthesized pyridine, pyrane, and pyrimidine derivatives, *Bioorg. Med. Chem.*, 2006, **14**(16), 5481–5488.
11 C. N. S. S. P. Kumar, D. K. Parida, A. Santhoshi, A. K. Kota, B. Sridhar and V. J. Rao, Synthesis and biological evaluation of tetrazole containing compounds as possible anticancer agents, *MedChemComm*, 2011, **2**(6), 486–492.
12 M. B. Labib, A. M. Fayez, E. L. S. El-Nahass, M. Awadallah and P. A. Halim, Novel tetrazole-based selective COX-2 inhibitors: Design, synthesis, anti-inflammatory activity, evaluation of PGE2, TNF-α, IL-6 and histopathological study, *Bioorg. Chem.*, 2020, **104**, 104308.
13 H. u Rashid, M. A. U. Martines, A. P. Duarte, J. Jorge, S. Rasool, R. Muhammad, N. Ahmad and M. N. Umar, Research developments in the syntheses, anti-inflammatory activities and structure–activity relationships of pyrimidines, *RSC Adv.*, 2021, **11**(11), 6060–6098.
14 A. Husain, C. S. Devi and B. Anupama, Synthesis, characterization, DNA binding, protein binding, antioxidant and anti microbial activity of tetrazole ring based complexes, *J. Mol. Struct.*, 2023, **1291**, 135963.
15 Y. Kotaiah, N. Harikrishna, K. Nagaraju and C. Venkata Rao, Synthesis and antioxidant activity of 1,3,4-oxadiazole tagged thieno[2,3-d]pyrimidine derivatives, *Eur. J. Med. Chem.*, 2012, **58**, 340–345.
16 S. I. Pretorius, W. J. Breytenbach, C. de Kock, P. J. Smith and D. D. N'Da, Synthesis, characterization and antimalarial activity of quinoline–pyrimidine hybrids, *Bioorg. Med. Chem.*, 2013, **21**(1), 269–277.
17 C. Gao, L. Chang, Z. Xu, X.-F. Yan, C. Ding, F. Zhao, X. Wu and L.-S. Feng, Recent advances of tetrazole derivatives as potential anti-tubercular and anti-malarial agents, *Eur. J. Med. Chem.*, 2019, **163**, 404–412.
18 V. Ivasiv, C. Albertini, A. E. Gonçalves, M. Rossi and M. L. Bolognesi, Molecular hybridization as a tool for designing multitarget drug candidates for complex diseases, *Curr. Top. Med. Chem.*, 2019, **19**(19), 1694–1711.
19 D. B. Upadhyay, J. Nogales, J. A. Mokariya, R. M. Vala, V. Tandon, S. Banerjee and H. M. Patel, One-pot synthesis of tetrahydropyrimidinecarboxamides enabling in vitro anticancer activity: a combinative study with clinically relevant brain-penetrant drugs, *RSC Adv.*, 2024, **14**(37), 27174–27186.
20 C. Viegas-Junior, A. Danuello, V. da Silva Bolzani, E. J. Barreiro and C. A. M. Fraga, Molecular hybridization: a useful tool in the design of new drug prototypes, *Curr. Med. Chem.*, 2007, **14**(17), 1829–1852.
21 C. A. M. Fraga, Drug hybridization strategies: before or after lead identification?, *Expert Opin. Drug Discovery*, 2009, **4**(6), 605–609.

22 S. Firoj Basha, T. N. Prasad, V. B. Gudise, V. S. Kumar, N. Mulakayala and S. Anwar, An efficient, multicomponent, green protocol to access 4,7-dihydrotetrazolo[1,5-a]pyrimidines and 5,6,7,9-tetrahydrotetrazolo[5,1-b]quinazolin-8(4H)-ones using PEG-400 under microwave irradiation, *Synth. Commun.*, 2019, **49**(22), 3181–3190.
23 R. Ghorbani-Vaghei, Z. Toghraei-Semiromi, M. Amiri and R. Karimi-Nami, One-pot synthesis of tetrazolo[1,5-a]-pyrimidines under solvent-free conditions, *Mol. Diversity*, 2013, **17**(2), 307–318.
24 S. Gorji, R. Ghorbani-Vaghei, Z. Toghraei-Semiromi and S. Alavinia, Synthesis of 5,8-Diaryl-5,7,8,9-Tetrahydropyrimido[5,4-e]Tetrazolo[1,5-a]Pyrimidin-6(4H)-One Derivatives Catalyzed by MNPs@SiO2-Pr-AP as a New Efficient Reusable Nanomagnetic Catalyst, *Polycycl. Aromat. Compd.*, 2021, **41**(9), 1849–1861.
25 P. Kour, V. P. Singh, B. Khajuria, T. Singh and A. Kumar, Al(III) chloride catalyzed multi-component domino strategy: Synthesis of library of dihydrotetrazolo[1,5-a]pyrimidines and tetrahydrotetrazolo[1,5-a]quinazolinones, *Tetrahedron Lett.*, 2017, **58**(44), 4179–4185.
26 T.-J. Li, C.-S. Yao, C.-X. Yu, X.-S. Wang and S.-J. Tu, Ionic Liquid–Mediated One-Pot Synthesis of 5-(Trifluoromethyl)-4,7-dihydrotetrazolo[1,5-a]pyrimidine Derivatives, *Synth. Commun.*, 2012, **42**(18), 2728–2738.
27 L. Suresh, P. Onkara, P. S. V. Kumar, Y. Pydisetty and G. V. P. Chandramouli, Ionic liquid-promoted multicomponent synthesis of fused tetrazolo[1,5-a]pyrimidines as α-glucosidase inhibitors, *Bioorg. Med. Chem. Lett.*, 2016, **26**(16), 4007–4014.
28 R. Ghiai, S. Alavinia, R. Ghorbani-Vaghei and A. Khazaei, Cu(II) Immobilized on Mesoporous Poly (Guanidine–Triazine–Sulfonamide) (PGTSA/Cu): A New Catalyst for the Synthesis of Tetrazolo[1,5-a]pyrimidines, *Appl. Organomet. Chem.*, 2025, **39**(2), e7831.
29 J. Jayakumar and S. Rajasekhara Reddy, Molecular oxygen-promoted sustainable synthesis of functionalized quinolines using catalytic glucose-derived ionic liquids and copper, *Org. Biomol. Chem.*, 2024, **22**(42), 8472–8479.
30 J. Jayakumar and S. R. Reddy, Chemoenzymatic Relay Synthesis of Quinolines: Laccase/TEMPO/D-Glucose-Based Ionic Salt/atm O2-Catalyzed Chemoselective Oxidation of 2-Aminobenzyl Alcohols, *ACS Sustainable Chem. Eng*, 2026, **14**(11), 5332–5344.
31 A. W. Bauer, W. M. M. Kirby, J. C. Sherris and M. Turck, Antibiotic Susceptibility Testing by a Standardized Single Disk Method, *Am. J. Clin. Pathol.*, 1966, **45**(4_ts), 493–496.
32 S. S. Bhalodiya, M. P. Parmar, S. Balachandran, C. D. Patel, A. Nandi, A. Das, M. K. Arumugam and H. M. Patel, [BMIM]OAc promoted one-pot synthesis of pyrazolo[4′,3′:5,6]pyrido[2,3-d]pyrimidin-5-ones and their antimicrobial activity, *RSC Adv.*, 2026, **16**(1), 488–500.
33 V. Jayaraman, M. K. Arumugam, S. Balachandran, L. Boopathy, S. Arumugam, J. Srirangaramasamy, S. Devanesan, A. Suresh and S. Sampath, Anticancer Effects of Monacolin X Against Human Liver Cancer Cell Line: Exploring the Apoptosis Using AO/EB and DCFHDA Fluorescent Staining, *Luminescence*, 2025, **40**(6), e70229.
34 N. Sirpu Natesh, M. Arumugam and G. Karanam, Apoptotic role of marine sponge symbiont Bacillus subtilis NMK17 through the activation of caspase-3 in human breast cancer cell line, *Mol. Biol. Rep.*, 2018, **45**(6), 2641–2651.
35 S. N. Nagabhishek, A. Madan Kumar, S. B,, A. Balakrishnan, Y. T. Katakia, S. Chatterjee and N. Nagasundaram, A marine sponge associated fungal metabolite monacolin X suppresses angiogenesis by down regulating VEGFR2 signaling, *RSC Adv.*, 2019, **9**(46), 26646–26667.
36 K. S. Suslick, Sonochemistry, *Science*, 1990, **247**(4949), 1439–1445.
37 G. Cravotto and P. Cintas, Power ultrasound in organic synthesis: moving cavitational chemistry from academia to innovative and large-scale applications, *Chem. Soc. Rev.*, 2006, **35**(2), 180–196.
38 P. Cintas and J.-L. Luche, Green chemistry. The sonochemical approach, *Green Chem.*, 1999, **1**(3), 115–125.
39 D. Prat, A. Wells, J. Hayler, H. Sneddon, C. R. McElroy, S. Abou-Shehada and P. J. Dunn, CHEM21 selection guide of classical- and less classical-solvents, *Green Chem.*, 2016, **18**(1), 288–296.
40 P. Anastas and J. C. Warner, *Green chemistry: theory and practice*, Oxford University Press: New York, NY, USA, 1998.